



RAF1 mediates the FSH signaling pathway as a downstream molecule to stimulate estradiol synthesis and secretion in mouse ovarian granulosa cells

Xuan Luo^{1#}, Hui Liu^{2#}, Hongzhou Guo¹, Longjie Sun¹, Kemian Gou², Sheng Cui^{1,2}

¹State Key Laboratory of Agrobiotechnology, College of Biological Sciences, China Agricultural University, Beijing, China; ²College of Veterinary Medicine, Yangzhou University, Yangzhou, China

Contributions: (I) Conception and design: S Cui; (II) Administrative support: K Gou; (III) Provision of study materials or patients: X Luo; (IV) Collection and assembly of data: X Luo; (V) Data analysis and interpretation: X Luo; (VI) Manuscript writing: All authors; (VII) Final approval of manuscript: All authors.

[#]These authors contributed equally to this work.

Correspondence to: Sheng Cui. State Key Laboratory of Agrobiotechnology, College of Biological Sciences, China Agricultural University, Beijing, China. Email: cuisheng@cau.edu.cn; Kemian Gou. College of Veterinary Medicine, Yangzhou University, Yangzhou, China. Email: gou@yzu.edu.cn.

Background: The v-raf-leukemia viral oncogene 1 (RAF1) plays an essential physiological role in reproduction and development through the mediation of steroid hormone synthesis. Follicle-stimulating hormone (FSH) signaling pathway was not involved in the majority of RAF1 studies, whether RAF1 takes part in the signaling events of gonadotropic hormones such as FSH in ovarian tissue is unknown.

Methods: The process is blocked by treating granulosa cells (GCs) with the RAF1 inhibitor, RAF709. Inhibition of RAF1 activity by RAF709 decreased extracellular regulated protein kinases (ERK) phosphorylation and suppressed the expression of the cytochrome P450 subfamily 19 member 1 (CYP19A1), which is a major rate-limiting enzyme that participates in the last step of E2 biosynthesis.

Results: We found that RAF1, acting as a downstream molecule, mediates FSH signalling to stimulate estradiol (E2) synthesis and secretion in mouse ovarian GCs. Gene expression of RAF1 was induced by FSH and the secretion of E2 increased into the bloodstream of mice and into the supernatant of primary GCs. Our *in vitro* and *in vivo* studies clearly illustrate RAF1 plays an important medium adjusting role in the FSH signaling pathway, and RAF1 acting as a downstream molecule to trigger ERK phosphorylation to stimulate GC E2 synthesis and secretion.

Conclusions: RAF1 plays a pivotal mediating role in the FSH signaling pathway by inducing the phosphorylation of ERK and promoting E2 synthesis.

Keywords: V-raf-leukemia viral oncogene 1 (RAF1); estradiol secretion; mouse ovarian granulosa cells

Submitted Dec 23, 2021. Accepted for publication Mar 16, 2022.

doi: 10.21037/atm-22-393

View this article at: <https://dx.doi.org/10.21037/atm-22-393>

Introduction

Estrogens are mainly secreted by granulosa cells (GCs) in the ovary and are essential for folliculogenesis (1,2), the development of secondary sex characteristics, and the maintenance of female reproductive function (3,4). Estrogens are derived from cholesterol by a tightly regulated

process which androgens are synthesized from cholesterol by luteinizing hormone (LH) responsive theca cells, followed by conversion to estrogens in follicle-stimulating hormone (FSH) exposed GCs, and involving the steroidogenic acute regulatory protein (StAR) which mediated transportation of cholesterol into the mitochondria (5,6), cytochromes

P450 and hydroxysteroid dehydrogenases which converts pregnenolone and progesterone to dehydroepiandrosterone and androstenedione (7). Among the regulatory enzymes, cytochrome P450 subfamily 19 member 1 (CYP19A1) is required for the final step in the biosynthesis of estradiol (E₂) which convert androgens to estrogens in GCs (8).

FSH acts as a key pituitary hormone that can promote follicles to secrete hormones (9), initiate signaling events in the ovary by binding to its receptor [follicle-stimulating hormone receptor (FSHR)] (10), and initiate complex signaling pathways (11). FSH has been shown to stimulate the phosphorylation of cyclic adenosine monophosphate (cAMP)-response element binding protein (CREB) and histone recombinant histone H3 (H3) in a protein kinase A (PKA)-dependent manner (12,13), and has also been shown to be associated with extracellular regulated protein kinases (ERK) by stimulating a protein tyrosine phosphatase (PTP) (14). However, the mechanisms of FSH-stimulated ERK phosphorylation to enhance estrogen secretion in GCs are still poorly understood.

At approximately 68 kDa, v-raf-leukemia viral oncogene 1 (RAF1) (also known as a C-RAF), at approximately 68 kDa, is the smallest isoform of the RAF kinases (15), and RAF1 kinase acts as a conserved signaling module transducing signals from the cell surface to the nucleus (16,17). Previous reports have shown that RAF1 receives extracellular signals and functions in the rat sarcoma (RAS) pathway to transmit signals to the downstream kinases, mitogen-activated protein kinase (MAPK) kinase (MEK) and ERK (18,19). In addition, RAF1 is activated by binding small G proteins of the RAS family to the N-terminal region of the RAF protein (20). Activated RAF1 subsequently activates MEK, MAP kinase (21), and other downstream kinases and transcription factors (22), and it has been reported that RAF is critical for steroidogenesis via ERK1/2, but the study depend on *in vitro* experiments only, the *in vivo* data were not available (23). Our recent study showed RAF1 to be a vital downstream signal in microRNA-regulating processes of pituitary hormones (24). These collective data suggest that RAF1 is involved in the regulation of steroid hormone synthesis, which led us to hypothesize that it is involved in the FSH signaling pathway to regulate E₂ synthesis and secretion in mouse GCs. We present the following article in accordance with the ARRIVE reporting checklist (available at <https://atm.amegroups.com/article/view/10.21037/atm-22-393/rc>).

Methods

Animals and treatments

Virgin adult wild-type female mice weighing 35–45 g in estrus were used for this study. Mice were purchased from Beijing HFK Bioscience Co. Ltd. (Beijing, China) and housed in a controlled temperature (20–25 °C) and humidity (60–65%) environment with a 12 h light/dark cycle and fed with basal diet and pure water. The animal experiment was approved by the ethics committee of China Agricultural University (No. AW80401202-3-1), in compliance with animal protection law of China and guidelines of China Agricultural University for Laboratory Animal Sciences and Animal Experimental Ethics Committee.

Mice were divided into four experimental groups to study RAF1 biological regulating functions induced by FSH. Treatment groups were given a single dose of FSH (10 IU/mouse) by intraperitoneal (IP) injection (25), and phosphate-buffered saline (PBS) was injected as control. RAF inhibitor RAF709 was injected to the treatment groups at 30 mg/kg and corn oil was injected to the controls as follows (26), (I) FSH group (FSH + corn oil, n=6), (II) FSH-RAF709 group (FSH + RAF709, n=6), (III) control group (PBS + corn oil, n=6), and (IV) RAF709 group (PBS + RAF709, n=6). We used vaginal lavage to collect vaginal cells for identifying the stages of the mouse estrous cycle (27).

Reagents and antibodies

All reagents and antibodies were commercially available, and included RAF709 (HY-100510, MCE); anti-Raf1 (ab137435, Abcam); FSHR(1:1,000; sc-13935, Santa); GAPDH (1:2,000; Am4300, Ambion); CYP19A1 antibody (1:2,000; BA3704, Boster); P-ERK antibody (1:1,000; CST); goat anti-rabbit IgG (1:5,000, ZB-2301; Zhongshan, Beijing, China); ECL Western blotting substrate (32209; Thermo Scientific, Waltham, MA); DMEM/F12 (D2906; Sigma); fetal bovine serum (FBS, Gibco); streptomycin (Sigma); corn oil (Sigma); FSH (Boleide, Beijing, China).

Isolation and culture of primary ovarian GCs

Mice were given pregnant mare serum gonadotropin (PMSG) (10 IU), and GCs were isolated and collected by follicle puncture as described (28). Primary ovarian GCs

were incubated in Dulbecco's Modified Eagle Medium/Nutrient Mixture F-12 (DMEM/F12) containing 10% fetal bovine serum (FBS) supplemented by 100 U/mL penicillin and 100 mg/mL streptomycin, and were cultured in a 5% CO₂ incubator with saturated humidity and a constant temperature of 37 °C. Primary ovarian GCs were collected and seeded in a 6-well plate at a density of 1×10⁶ cells. When cells attached and grew on the cell culture dishes reaching approximately 70% confluence, the culture medium was changed to that without FBS for starvation. After starvation for 24 h, the cells were treated with FSH (100 ng/mL) (29). In experiments, GCs were pretreated with RAF1 inhibitor RAF709 (5 nM) 6 h before hormone treatment (26).

The collected primary ovarian GCs were divided into four groups according to the treatment method: (I) a FSH group (FSH + dimethyl sulfoxide (DMSO), n=6), untreated GCs in the presence of FSH; (II) a FSH-RAF709 group (FSH + RAF709, n=6), GCs were pretreated with inhibitor before induction by FSH; (III) a control group (PBS + DMSO, n=6), GCs plated in normal medium without FSH induction; and (IV) a RAF709 group (PBS + RAF709, n=6), GCs were pretreated with inhibitor in normal medium without FSH induction.

RNA extraction and real-time quantitative PCR (RT-qPCR) analysis

The ovary samples were dissected and extracted by grinding under liquid nitrogen. Total RNA was extracted from the tissue and Trizol reagent (TaKaRa Biotechnology, Dalian, China) following the manufacturer's instructions and after quantification by spectrophotometry, the purified total RNA (1 µg) was used as a template for cDNA synthesis. RNA was supplemented with the appropriate amount of DEPC H₂O to make the total volume up to 6 µL, while Oligo (dT) was added and gently mixed and heated at 72 °C for 5 min then immediately cooled to 0–4 °C for at least 5 min. The following reagents were added: MLV, dNTP, and RNA safe (Promega), and incubated for 1 h at 42 °C. Glyceraldehyde-3-phosphate dehydrogenase (GAPDH) was assayed as an internal control, and RT-qPCR was performed using a standard Takara SYBR Premix Ex Taq protocol on an Applied Biosystems 7500 Real-Time PCR system (Applied Biosystems). GAPDH expression levels were used for data normalization and the relative abundance of genes was determined using ABI PRISM 7500 equipped software (Applied Biosystems).

The relative product levels were quantified using the 2^{-ΔΔCt} method, and the primers for RT-qPCR analyses were as follows: *Raf-1*. Forward primer *GCTAATTGACATTGCCCGACA*; Reverse primer *TTCAACCTGCTGAGAACCAC*. *Gapdh*. Forward primer *GGTTGTCTCCTGCGACTTCA*; Reverse primer *GGGTGGTCCAGGGTTTCTTA*.

Western blotting (WB)

Ovaries were lysed with RIPA buffer (C1053, Applygen, Beijing, China) containing 1 mM phenylmethanesulfonyl fluoride (PMSF; 78830, Sigma). The protein concentration of each sample was quantitated by the BCA assay reagent (HX18651, Huaxingbio, Beijing, China), and equal amounts of proteins were normalized to 30 ng and the loading buffer size calculated. Samples were electrophoresed on SDS-PAGE 5% stacking gel at 80 V for 30 min and 12% separating gel at 120 V for 45 min using a polyvinylidene fluoride (PVDF) membrane (IPVH00010, Millipore, Billerica, MA, USA). The membrane was soaked in methanol and the target proteins were transferred to a PVDF membrane at 250 mA for 1.5 h under constant current (mA). Non-fat dried milk 5% (wt/vol) in Tris-buffered saline (TBS) was used to block the membranes for 2 h at room temperature, which were then incubated with RAF1 antibody (1:2,000; ab137435, Abcam), CYP19A1 antibody (1:1,000; BA3704; Boster), P-ERK antibody (1:1,000; 4370T; Cell Signaling Technologies), ERK1/2 (1:1,000; A4782; Abclonal), and internal control GAPDH (1:2,000, PA5-85074; Ambion) overnight at 4 °C. The membrane was washed in TBST (0.1% Tween-20 in TBS) every 10 min and incubated with horseradish peroxidase-conjugated goat anti-rabbit IgG (1:5,000, ZB-2301; Zhongshan) for 1 h at room temperature. After 30 min in TBST, the membrane was treated with ECL Western blotting substrate (32209; Thermo Scientific, Waltham, MA, USA) at room temperature, from 30 sec to 20 min to detect the signal protein.

Immunohistochemistry

Ovarian tissue sections in paraffin were dewaxed in ethanol and soaked in 3% H₂O₂ (vol/vol) for 20 min to eliminate endogenous peroxidase activity. Samples were microwaved in 0.01 M sodium citrate buffer on high power for 15 min and washed with PBS, and normal goat serum (10%) was added for 1 h at room temperature to eliminate background nonspecific coloring. The sections were incubated with

RAF1 antibody (1:150; HY-100510, Abcam) overnight at 4 °C. The slides were washed with PBS three times, and biotinylated goat anti-rabbit IgG (1:200; 11-065-14, Jackson) was incubated for 2 h at 37 °C. HRP-conjugated streptavidin (1:200; 016-030-084, Jackson) was used for incubating at room temperature, and Diaminobenzidine (DAB) was added for color rendering, with the color development degree controlled under the microscope. The appearance of brown staining was considered a positive reaction.

Immunofluorescence

GCs grown on glass slides to 95–100% confluence were fixed in 4% paraformaldehyde for 25 min. Cells were then washed with PBS for 10 min and permeabilized with 0.1% Triton X-100 (Sigma), then blocked using 10% normal goat serum in TBS for 1 h at room temperature. The cells were incubated with RAF1 antibodies (1:200, diluted with 1% TBS) and placed in a wet box overnight at 4 °C. The slides were washed twice for 5 min each time by PBS, followed by incubation with the FITC-labeled goat anti-rabbit IgG (GAR-FITC, ZF-0311, Zhongshan) for 60 min, then the nuclei were dyed with 4',6-diamidino-2-phenylindole (DAPI, 1:1,000, D8417; Sigma) for 15 min. Nonimmune rabbit IgG was used as a negative control. Slides were washed with PBS three times to remove the excess DAPI.

Radioimmunoassay

The concentrations of E₂ in mouse serum and culture media were measured by radioimmunoassay using reagents provided by the Beijing North Institute of Biological Technology (Beijing, China). Experiments were repeated three times. The minimum detectable concentration was 5 pg/mL for estradiol, and for each radioimmunoassay, the intra- and interassay coefficients of variation were less than 10% and 15%, respectively.

Statistical analysis

All data were analyzed by GraphPad Prism 6 software (GraphPad Software Inc., San Diego, CA, USA) and presented as means ± SEM. One-way analysis of variance (ANOVA) and Duncan's tests were used to analyze the main effects of treatments and P<0.05 was considered as indicating significant differences between treatment groups. WB grayscale images were converted to peak and their size

measured by ImageJ software v1.8.0.

Results

Raf1 was expressed in mouse ovary at estrus stage and located in the GCs

We firstly examined Raf-1 mRNA and protein levels in the ovary at different stages of the estrus cycle by PCR (RT-qPCR) and WB analysis. The results showed that RAF1 expression was highest at estrus both at gene and protein levels and significantly higher (P<0.05) than at proestrus, metestrus, and diestrus stages, between which there was no significant difference (*Figure 1A,1B*). Furthermore, we located RAF1 expression by using immunofluorescence staining in cultured GCs, and the results showed that RAF1 positive staining was observed in GCs (*Figure 1C*). We also performed immunohistochemistry, and the results (*Figure 1D*) showed that RAF1 positive staining was observed in the most GCs. Meanwhile, the RAF1 antibodies were replaced with anti-rabbit IgG for negative control (*Figure 1E*), the results were similar to the immunofluorescence staining found in the cultured GCs. These data suggest that RAF1 might be involved in regulating ovarian function and antibodies.

RAF1 participates in regulating E2 secretion

To identify whether RAF1 was involved in regulating estradiol synthesis in mouse ovaries, 30 mg/kg of the RAF1 inhibitor, RAF 709, was dissolved in vegetable oil and injected intraperitoneally into mice, while control mice received vegetable oil only. Mice were sacrificed after injection, and ovaries were harvested for measurement of RAF1 gene expression, while blood samples were collected for serum E₂ measurement. RAF709 treatment resulted in a dose-dependent decrease in E₂ concentrations in the culture supernatant fluid, and at 5 nM RAF709, E₂ levels decreased by 42.3% (*Figure 2A*). In addition, in GCs cultured with 0 (control), 0.5, 1, 2, or 5 nM RAF709 for 6 h, RAF1 expression at both the gene and protein levels showed RAF709 effectively downregulated *Raf-1* mRNA and RAF1 protein levels in GCs in a dose-responsive manner (*Figure 2B,2C*), while at 5 nM RAF709, *Raf-1* mRNA and protein levels were reduced obviously (*Figure 2B,2C*). After RAF709 treatment, the serum E₂ levels significantly decreased compared with the controls (*Figure 2D*) *in vivo*. The RT-qPCR and WB results showed that *RAF1* gene and

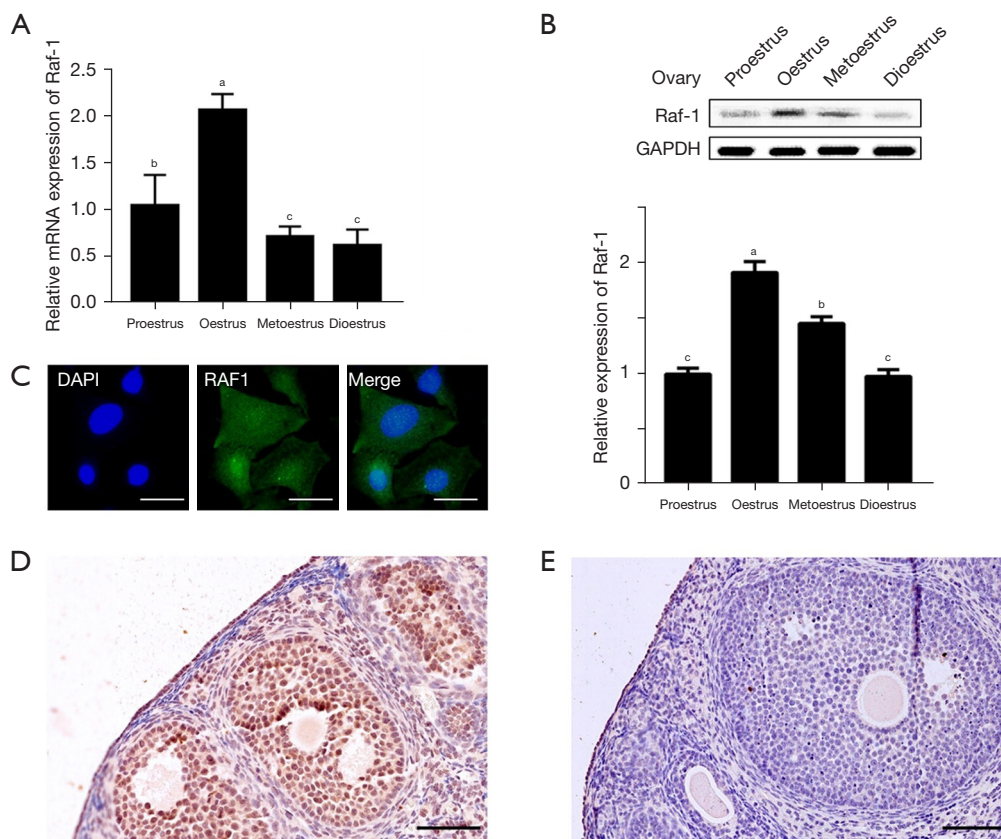


Figure 1 RAF1 was expressed in ovarian GCs of mice during estrus. (A) RT-PCR was used to analyze Raf-1 mRNA expression in the ovaries during each cycle of mice. (B) RAF1 protein abundances from ovary tissues at the different estrus cycle stages were analyzed by WB with GAPDH as the internal reference. The different letters above the error bars indicate a significant difference between results at the different estrus stages ($P < 0.05$). At least four adult wild female mice were used at each timepoint (proestrus, oestrus, metoestrus, and dioestrus). (C) Immunofluorescence technique was used to observe RAF1 location inside the primary ovarian GCs *in vitro*. Blue fluorescence displayed the hallmarks of the GC nucleus by DAPI staining, scale bar = 20 μm , and green fluorescence indicates RAF1-positive signal staining. (D,E) Mouse ovarian samples were incubated with RAF1 antibodies and antibodies were replaced with anti-rabbit IgG for negative control. The localization of RAF1 proteins in ovary tissue was performed by immunohistochemical staining assay. Selectively staining brown demonstrates RAF1-positive signals. The morphology of mouse GCs was observed under high magnification microscope $\times 100$, scale bar = 50 μm .

protein levels decreased evidently (Figure 2E,2F). These *in vivo* and *in vitro* results demonstrate that RAF1 functions to enhance E_2 synthesis and secretion in mouse ovary GCs.

RAF1 mediates estradiol secretion through phosphorylation of ERK in mouse ovary GCs

To confirm our hypothesis that RAF1 was involved in the FSH signaling pathway stimulating E_2 synthesis, cultured GCs were treated with FSH, RAF709, or FSH+RAF709, and protein levels of FSHR, RAF1, ERK-P, and CYP19A1 and the E_2 concentration in the culture medium were

assayed. The results confirmed that FSH significantly increased FSHR and E_2 levels (Figure 3A), whereas RAF709 treatment blocked RAF1, ERK-P, and CYP19A1 expression, and E_2 levels (Figure 3B-3E) but had no significant effect on FSHR compared with the controls. These data suggest that signals between FSH and E_2 are blocked when the RAF1 is blocked by inhibitor in mouse primary ovarian GCs, and RAF1 acts as a downstream molecule to mediate the FSH signaling pathway, stimulating E_2 synthesis through phosphorylation of ERK.

To confirm the above *in vitro* results in the cultured GC, *in vivo* experiments were performed by injecting exogenous

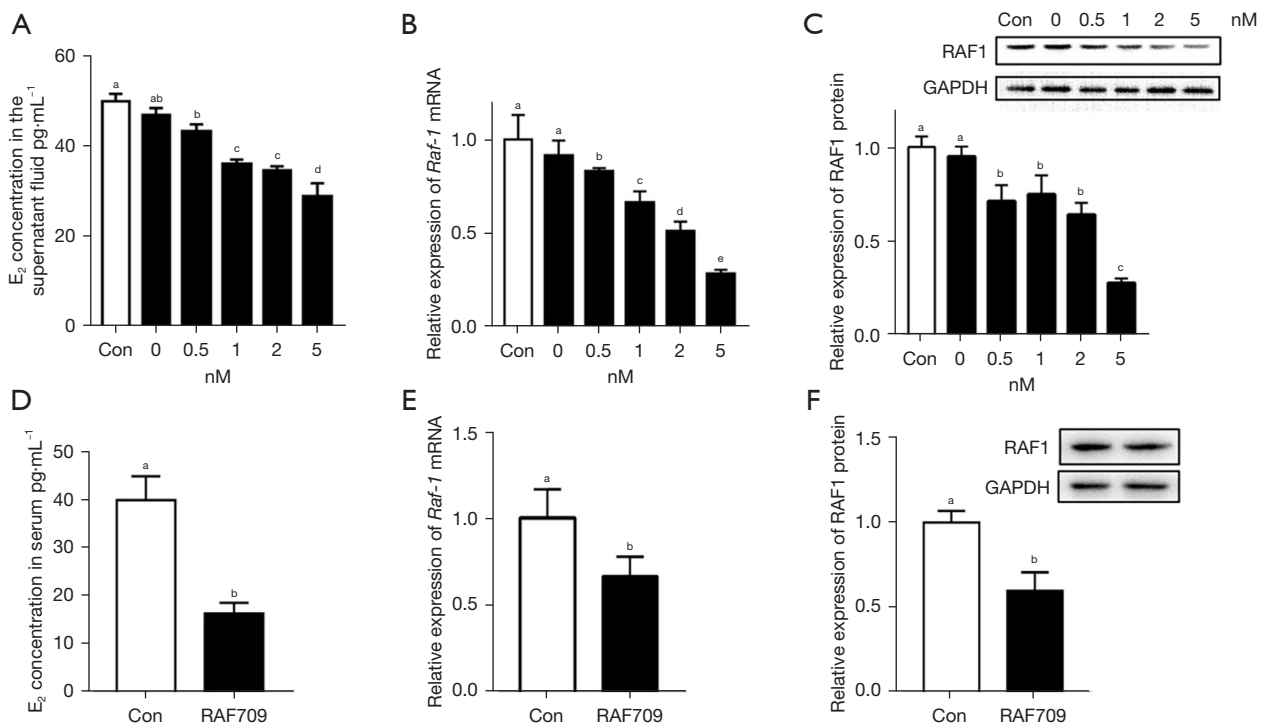


Figure 2 RAF1 inhibition blocked the secretion of E₂. (A) GCs were treated by inhibitor with various concentration and each treatment had six replicates, E₂ concentrations in the culture supernatant from GCs were examined by RIA. (B) The GCs were collected, and their Raf-1 mRNA expression was analyzed using RT-PCR. (C) RAF1 protein expression data in GCs were quantified using ImageJ software. (D) RAF inhibitor was injected into wild adult female rats and corn oil was injected into the controls. Each group had three replicates, and RIA was used to examine the contents of serum E₂ levels. (E) The Raf-1 mRNA expression in ovaries was analyzed using RT-PCR. (F) RAF1 protein expression data in ovaries was quantified using ImageJ software. GAPDH was used as an internal control. The same letters indicate the difference is not significant, and different letters indicate that the difference is significant (P<0.05). The values are the means ± SEM of three independent experiments. Different letters (a, b, c, and d) between two bars show a significant difference (a versus b, b versus c, and c versus d: P <0.05).

FSH, RAF709, or FSH+RAF709 into four groups of mice. The results showed that the changes in FSHR gene expression were not synchronous with changes in the RAF1 protein (Figure 4A), but the levels of RAF1, ERK-P, and CYP19A1 protein expression decreased significantly after injection of RAF709 (Figure 4B-4D), and E₂ levels in serum were much reduced compared with controls (Figure 4E). These *in vitro* and *in vivo* results suggest that RAF1 acts with the downstream molecules of the FSH signaling pathway to affect the synthesis and secretion of E₂.

Model of RAF1 function in mouse ovarian GC estradiol secretion

Our *in vitro* and *in vivo* studies clearly illustrate RAF1 plays an important medium adjusting role in the E₂ regulation of the FSH signaling pathway.

Discussion

The present study shows that FSH stimulates E₂ synthesis and secretion via the FSH signaling pathway in mouse GCs. Previous reports have shown RAF is involved in the regulation of steroid hormone synthesis via ERK1/2, or affected the functions of steroid hormones and their receptors (23,30). We have previously shown that miR-7 mediated the effects of GnRH on gonadotropin secretion by the mouse pituitary gland, and that RAF1 was a vital downstream signal in processes regulated by miR-7 (24). The present study demonstrates RAF1 acts as a member of the FSH pathway to trigger ERK phosphorylation and stimulate GC E₂ synthesis and secretion events. Our results show that RAF1 is highly expressed in ovarian GCs during estrus and the expression intensity and pattern of RAF1 genes are similar to the estrus cycle period wave change.

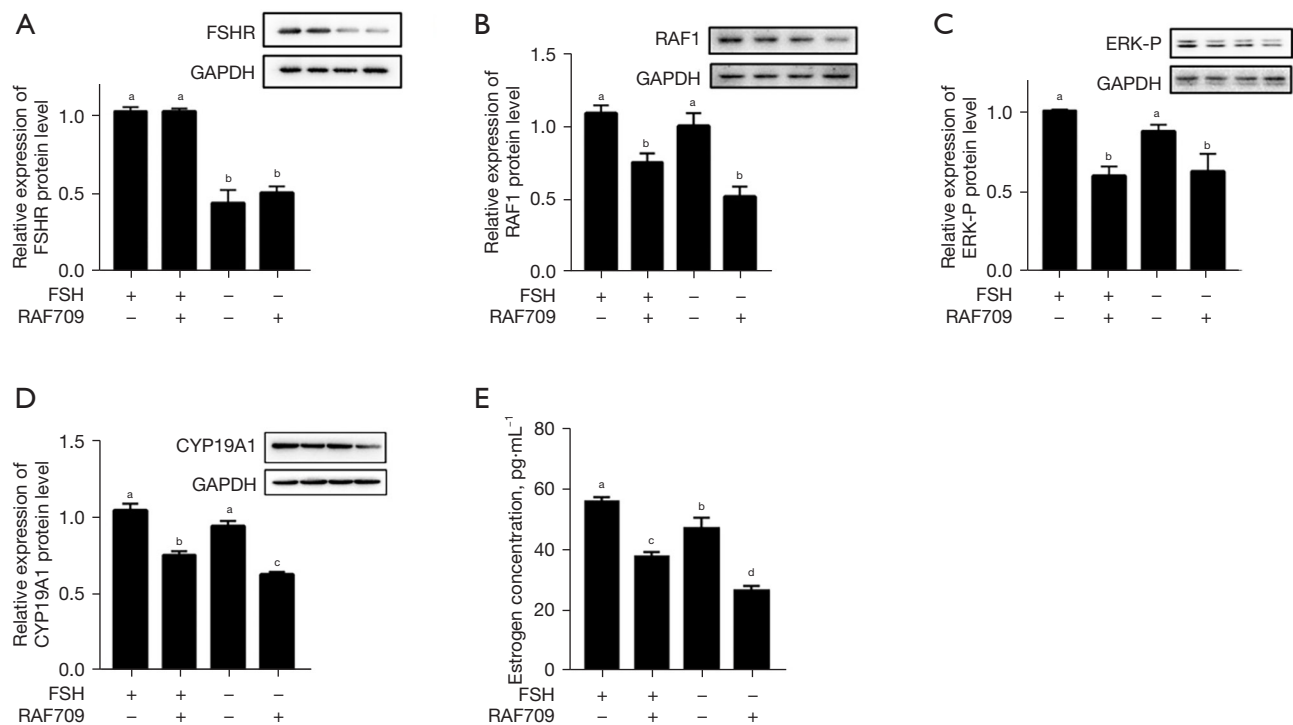


Figure 3 RAF1 involved in estradiol secretions by activating ERK phosphorylation. The primary ovarian GCs were treated with RAF709, 5 nM for 6 h then induced by FSH (100 ng/mL) for 24 h. (A-D) The protein expression ratios of FSHR, RAF1, ERK-P, and CYP19A1 were respectively detected by WB, and the protein ratios were analyzed in treatment groups relative to the GAPDH protein abundance. (E) Estradiol content was measured in each treatment group by RIA. The values are the means \pm SEM of three independent experiments. Different letters indicate a significant difference between the compared groups ($P < 0.05$). Different letters (a, b, c, and d) between two bars show a significant difference (a versus b, b versus c, and c versus d: $P < 0.05$).

Our *in vitro* and *in vivo* results suggest there might be an E_2 link with RAF1.

We assessed RAF1 plays an important medium adjusting role in the E_2 regulation of the FSH signaling pathway by giving mice and cultured cells an effective selective RAF1 inhibitor, RAF709, which can suppress RAS-driven cascade reactions and block the signal transduction pathway of mitogen-activated protein kinases (MAPK) (26,31). Our results showed that RAF709 decreased E_2 concentrations in a dose-dependent manner such that 5 nM RAF709 decreased E_2 levels by 42.3% *in vitro*, which agreed with previous studies in which E_2 secretion levels fell by almost half when RAF was suppressed (23). A number of studies suggest that RAF can affect the proliferation of cells through influencing the distribution of the cell cycle (32-34), and we speculated that the significant and rapid change of E_2 levels was caused by GC proliferation. Our flow cytometry analysis showed that RAF709 did not induce suppression of the cell cycle stage *in vitro* (Figure S1), but rather affected

the activity of E_2 synthase, which made us speculate RAF1 could regulate aromatase (estrogen synthetase) activity such as CYP19A1 through the ERK signaling pathways (35,36). Published results showed that upregulated miR-497 levels would inhibit the expression of RAF1 and suppress phosphorylation status of MEK1 and ERK1. In addition, our results showed that inhibition of RAF1 suppresses CYP19A1 expression by phosphorylation of ERK, which is consistent with the findings that the RAF-ERK pathway plays a vital role in mediating steroidogenesis (23).

FSH functions via the FSHR (37) and FSH supplement could promote E_2 production (25,38). We blocked the activity of RAF1 in the presence of FSH to study whether it could reduce E_2 secretion, and our results demonstrated that RAF709 blocked RAF1 expression and decreased secretion of E_2 by suppressing the phosphorylation status of ERK, CYP19A1 expression. These observations suggest that RAF1 plays an important medium adjusting role in the E_2 secretion of the FSH signaling pathway, although

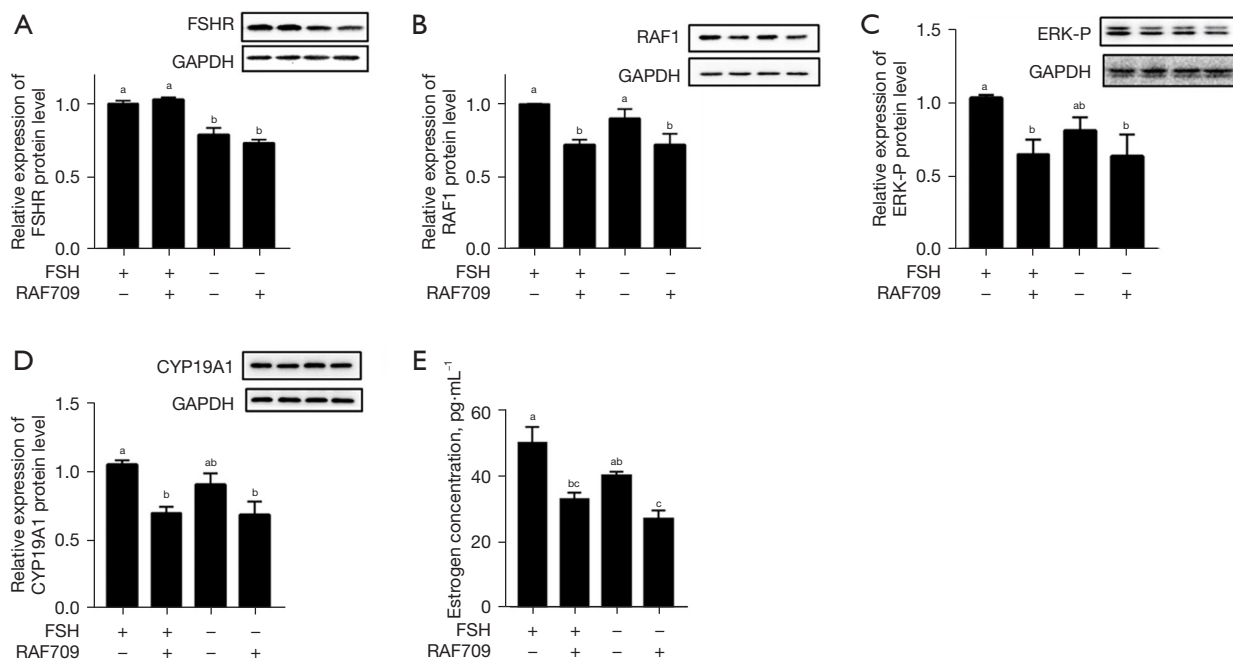


Figure 4 RAF1 acts as a downstream molecule to mediate the FSH signaling pathway to stimulate E₂ synthesis and secretion *in vivo*. Mice were given a single dose of FSH (10 IU/mouse) by intraperitoneal injection, and after 24 h, were injected with RAF709. After 24 h, blood samples of mice were collected for E₂ content. Vegetable oils were used as RAF709 reference substance and PBS served as a comparison with FSH for first injections. (A-D) FSHR, RAF1, ERK-P, and CYP19A1 protein expression in each treatment group detected by WB. Data were analyzed by GraphPad Prism version 5. (E) Estradiol content in mouse serum was measured in each treatment group by RIA. The same letters indicate the difference is not significant, and different letters indicate the difference is significant (P<0.05). The values are the means ± SEM of three independent experiments. Different letters (a, b, c, and d) between two bars show a significant difference (a versus b, b versus c, and c versus d: P < 0.05).

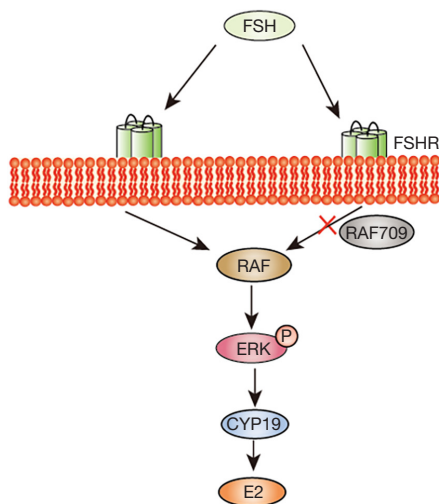


Figure 5 RAF1 is involved in the FSH signaling pathway to stimulate E₂ synthesis in mouse ovaries. RAF709, RAF1 inhibitor; ERK, extracellular signal-regulated kinase; CYP19, cytochrome P450 family 19.

further work is needed to test whether RAF1 affects FSH-R function in the ovary.

A better understanding of RAF1 may be helpful to elucidate the mechanism of steroid biosynthesis. RAF1 may be an effective factor in the regulation of hormone secretion and in understanding the structure and function of the female reproductive system.

In conclusion, our data demonstrate that RAF1 affected E₂ level in mouse ovarian GCs by ERK phosphorylation and aromatase CYP19A1 in the FSH signaling pathway, although the related molecular mechanisms need to be elucidated in future studies (Figure 5).

Acknowledgments

Funding: This work was supported by the National Key Research and Development Program of China (No. 2018YFC1003800).

Footnote

Reporting Checklist: The authors have completed the ARRIVE reporting checklist. Available at <https://atm.amegroups.com/article/view/10.21037/atm-22-393/rc>

Data Sharing Statement: Available at <https://atm.amegroups.com/article/view/10.21037/atm-22-393/dss>

Conflicts of Interest: All authors have completed the ICMJE uniform disclosure form (available at <https://atm.amegroups.com/article/view/10.21037/atm-22-393/coif>). The authors have no conflicts of interest to declare.

Ethical Statement: The authors are accountable for all aspects of the work in ensuring that questions related to the accuracy or integrity of any part of the work are appropriately investigated and resolved. The animal experiment was approved by the ethics committee of China Agricultural University (No. AW80401202-3-1), in compliance with animal protection law of China and guidelines of China Agricultural University for Laboratory Animal Sciences and Animal Experimental Ethics Committee.

Open Access Statement: This is an Open Access article distributed in accordance with the Creative Commons Attribution-NonCommercial-NoDerivs 4.0 International License (CC BY-NC-ND 4.0), which permits the non-commercial replication and distribution of the article with the strict proviso that no changes or edits are made and the original work is properly cited (including links to both the formal publication through the relevant DOI and the license). See: <https://creativecommons.org/licenses/by-nc-nd/4.0/>.

References

- Prasasya RD, Mayo KE. Notch Signaling Regulates Differentiation and Steroidogenesis in Female Mouse Ovarian Granulosa Cells. *Endocrinology* 2018;159:184-98.
- Lei L, Jin S, Mayo KE, et al. The interactions between the stimulatory effect of follicle-stimulating hormone and the inhibitory effect of estrogen on mouse primordial folliculogenesis. *Biol Reprod* 2010;82:13-22.
- Jdidi H, Kouba FG, Aoiadni N, et al. Effects of estrogen deficiency on liver function and uterine development: assessments of *Medicago sativa*'s activities as estrogenic, anti-lipidemic, and antioxidant agents using an ovariectomized mouse model. *Arch Physiol Biochem* 2021;127:170-81.
- Ling S, Dai A, Dilley RJ, et al. Endogenous estrogen deficiency reduces proliferation and enhances apoptosis-related death in vascular smooth muscle cells: insights from the aromatase-knockout mouse. *Circulation* 2004;109:537-43.
- Mizrachi D, Auchus RJ. Androgens, estrogens, and hydroxysteroid dehydrogenases. *Mol Cell Endocrinol* 2009;301:37-42.
- Tsujishita Y, Hurley JH. Structure and lipid transport mechanism of a StAR-related domain. *Nat Struct Biol* 2000;7:408-14.
- Miller WL, Auchus RJ. The molecular biology, biochemistry, and physiology of human steroidogenesis and its disorders. *Endocr Rev* 2011;32:81-151.
- Labrie F, Luu-The V, Lin SX, et al. Role of 17 beta-hydroxysteroid dehydrogenases in sex steroid formation in peripheral intracrine tissues. *Trends Endocrinol Metab* 2000;11:421-7.
- Heitman LH, Ijzerman AP. G protein-coupled receptors of the hypothalamic-pituitary-gonadal axis: a case for GnRH, LH, FSH, and GPR54 receptor ligands. *Med Res Rev* 2008;28:975-1011.
- Thomas RM, Nechamen CA, Mazurkiewicz JE, et al. The adapter protein APPL1 links FSH receptor to inositol 1,4,5-trisphosphate production and is implicated in intracellular Ca(2+) mobilization. *Endocrinology* 2011;152:1691-701.
- Kara E, Crépieux P, Gauthier C, et al. A phosphorylation cluster of five serine and threonine residues in the C-terminus of the follicle-stimulating hormone receptor is important for desensitization but not for beta-arrestin-mediated ERK activation. *Mol Endocrinol* 2006;20:3014-26.
- Carlone DL, Richards JS. Functional interactions, phosphorylation, and levels of 3',5'-cyclic adenosine monophosphate-regulatory element binding protein and steroidogenic factor-1 mediate hormone-regulated and constitutive expression of aromatase in gonadal cells. *Mol Endocrinol* 1997;11:292-304.
- Salvador LM, Park Y, Cottom J, et al. Follicle-stimulating hormone stimulates protein kinase A-mediated histone H3 phosphorylation and acetylation leading to select gene activation in ovarian granulosa cells. *J Biol Chem* 2001;276:40146-55.
- Cottom J, Salvador LM, Maizels ET, et al. Follicle-stimulating hormone activates extracellular signal-regulated kinase but not extracellular signal-regulated kinase kinase through a 100-kDa phosphotyrosine

- phosphatase. *J Biol Chem* 2003;278:7167-79.
15. Wellbrock C, Karasarides M, Marais R. The RAF proteins take centre stage. *Nat Rev Mol Cell Biol* 2004;5:875-85.
 16. Zhang W, Liu HT. MAPK signal pathways in the regulation of cell proliferation in mammalian cells. *Cell Res* 2002;12:9-18.
 17. Raman M, Chen W, Cobb MH. Differential regulation and properties of MAPKs. *Oncogene* 2007;26:3100-12.
 18. Ghousein A, Mosca N, Cartier F, et al. miR-4510 blocks hepatocellular carcinoma development through RAF1 targeting and RAS/RAF/MEK/ERK signalling inactivation. *Liver Int* 2020;40:240-51.
 19. Dougherty MK, Müller J, Ritt DA, et al. Regulation of Raf-1 by direct feedback phosphorylation. *Mol Cell* 2005;17:215-24.
 20. Chong H, Vikis HG, Guan KL. Mechanisms of regulating the Raf kinase family. *Cell Signal* 2003;15:463-9.
 21. Dent P, Haser W, Haystead TA, et al. Activation of mitogen-activated protein kinase kinase by v-Raf in NIH 3T3 cells and in vitro. *Science* 1992;257:1404-7.
 22. Vojtek AB, Hollenberg SM, Cooper JA. Mammalian Ras interacts directly with the serine/threonine kinase Raf. *Cell* 1993;74:205-14.
 23. Xu D, He H, Jiang X, et al. Raf-ERK1/2 signalling pathways mediate steroid hormone synthesis in bovine ovarian granulosa cells. *Reprod Domest Anim* 2019;54:741-9.
 24. He J, Zhang J, Wang Y, et al. MiR-7 Mediates the Zearalenone Signaling Pathway Regulating FSH Synthesis and Secretion by Targeting FOS in Female Pigs. *Endocrinology* 2018;159:2993-3006.
 25. Tu X, Liu M, Tang J, et al. The ovarian estrogen synthesis function was impaired in Y123F mouse and partly restored by exogenous FSH supplement. *Reprod Biol Endocrinol* 2018;16:44.
 26. Nishiguchi G, Rico AC, Tanner HR, et al. Design and Discovery of N-(2-Methyl-5'-morpholino-6'-((tetrahydro-2H-pyran-4-yl)oxy)-[3,3'-bipyridin]-5-y 1)-3-(trifluoromethyl)benzamide (RAF709): A Potent, Selective, and Efficacious RAF Inhibitor Targeting RAS Mutant Cancers. *J Med Chem* 2017;60:4869-81.
 27. McLean AC, Valenzuela N, Fai S, et al. Performing vaginal lavage, crystal violet staining, and vaginal cytological evaluation for mouse estrous cycle staging identification. *J Vis Exp* 2012;(67):e4389.
 28. Zhang C, Gong P, Ye Y, et al. NF- κ B-vimentin is involved in steroidogenesis stimulated by mono-butyl phthalate in primary cultured ovarian granulosa cells. *Toxicol In Vitro* 2017;45:25-30.
 29. Heng D, Wang Q, Ma X, et al. Role of OCT4 in the Regulation of FSH-Induced Granulosa Cells Growth in Female Mice. *Front Endocrinol (Lausanne)* 2019;10:915.
 30. Savtekin G, Serakinci N, Erzik C, et al. Effects of Circadian Rhythm Hormones Melatonin and 5-Methoxytryptophol on COXs, Raf-1 and STAT3. *Int J Pharmaco* 2018;14:787-95.
 31. Shao W, Mishina YM, Feng Y, et al. Antitumor Properties of RAF709, a Highly Selective and Potent Inhibitor of RAF Kinase Dimers, in Tumors Driven by Mutant RAS or BRAF. *Cancer Res* 2018;78:1537-48.
 32. Zhou Y, Hu J. Evodiamine Induces Apoptosis, G2/M Cell Cycle Arrest, and Inhibition of Cell Migration and Invasion in Human Osteosarcoma Cells via Raf/MEK/ERK Signalling Pathway. *Med Sci Monit* 2018;24:5874-80.
 33. Ye CY, Zheng CP, Ying WW, et al. Up-regulation of microRNA-497 inhibits the proliferation, migration and invasion but increases the apoptosis of multiple myeloma cells through the MAPK/ERK signaling pathway by targeting Raf-1. *Cell Cycle* 2018;17:2666-83.
 34. Ding M, Weng XQ, Sheng Y, et al. Dasatinib synergizes with ATRA to trigger granulocytic differentiation in ATRA resistant acute promyelocytic leukemia cell lines via Lyn inhibition-mediated activation of RAF-1/MEK/ERK. *Food Chem Toxicol* 2018;119:464-78.
 35. Liu J, Li X, Yao Y, et al. miR-1275 controls granulosa cell apoptosis and estradiol synthesis by impairing LRH-1/CYP19A1 axis. *Biochim Biophys Acta Gene Regul Mech* 2018;1861:246-57.
 36. Tao L, Zhang CY, Guo L, et al. MicroRNA-497 accelerates apoptosis while inhibiting proliferation, migration, and invasion through negative regulation of the MAPK/ERK signaling pathway via RAF-1. *J Cell Physiol* 2018;233:6578-88.
 37. Chitnis SS, Selvaakumar C, Jagtap DD, et al. Interaction of follicle-stimulating hormone (FSH) receptor binding inhibitor-8: a novel FSH-binding inhibitor, with FSH and its receptor. *Chem Biol Drug Des* 2009;73:637-43.
 38. Zhao H, Ge J, Wei J, et al. Effect of FSH on E2/GPR30-mediated mouse oocyte maturation in vitro. *Cell Signal* 2020;66:109464.

Cite this article as: Luo X, Liu H, Guo H, Sun L, Gou K, Cui S. RAF1 mediates the FSH signaling pathway as a downstream molecule to stimulate estradiol synthesis and secretion in mouse ovarian granulosa cells. *Ann Transl Med* 2022;10(6):314. doi: 10.21037/atm-22-393

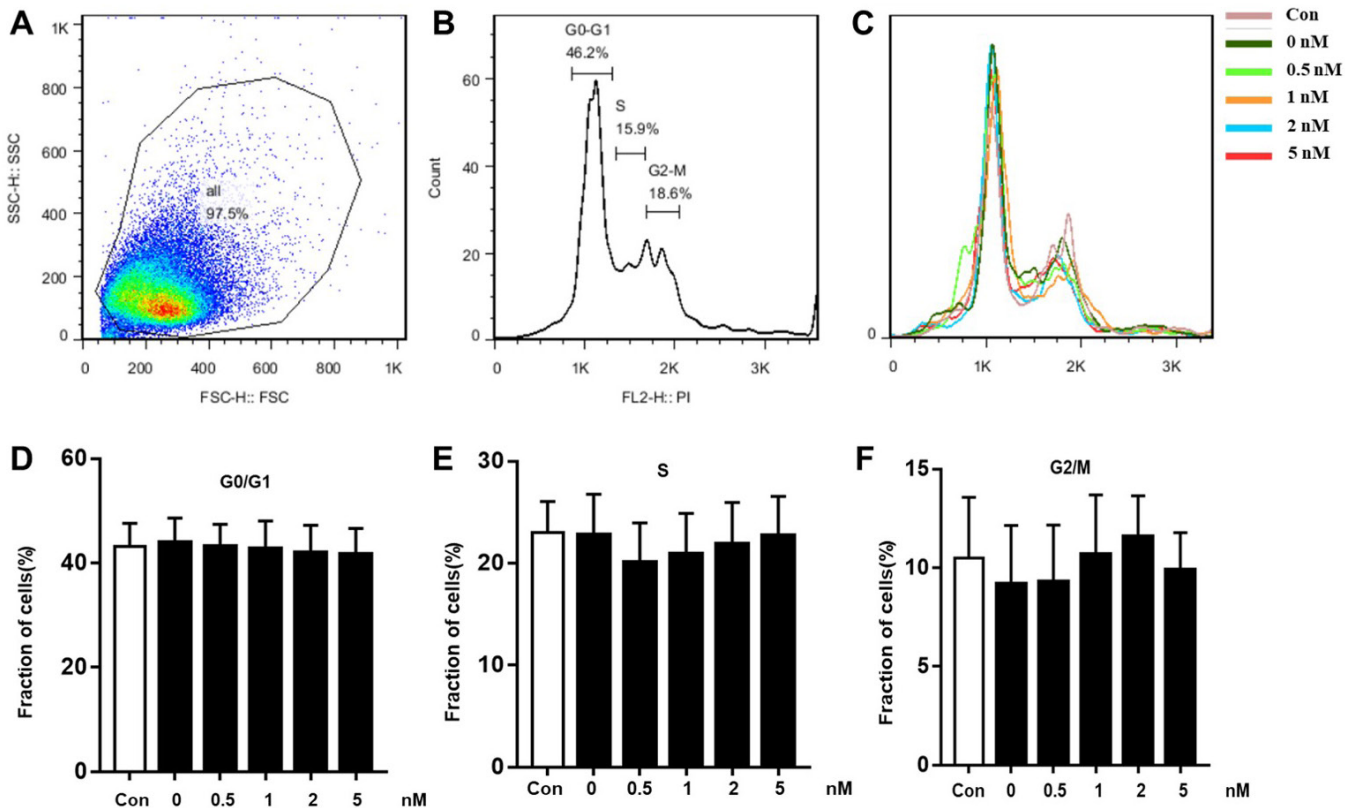


Figure S1 Cell viability was measured in GCs by staining the cells with Annexin V and propidium Iodide solution. (A) These gates cover about 97.5% of all events observed. (B) PI histogram of control cells and different stage of the cell cycle: G1 cells (first peak), G2 cells (second peak) and S-phase region lies between the two major peaks. (C) The histogram of inhibitor treated cells. (D-F) the percentage of treated GCs at each stage (G0-G1, S and G2-M) were calculated. GCs were labeled fluorescently for detection by Annexin V-PI staining (BD, Cat. No. 556547). A minimum of 10,000 cells within the gated region were analyzed, GCs were kept in dark till assessment and were analyzed by flow cytometer within one hour. Cells at FSC-SSC (forward scatter-side scatter) plot were gated according to untreated cells, and the percentage of treated GCs at each stage (G0-G1, S and G2-M) were calculated. We draw the picture by GraphPad Prism 6 software (GraphPad Software Inc., San Diego, CA, USA). One-way analysis of variance (ANOVA) and Duncan's tests were used to analyze the data. $P < 0.05$ was considered as indicating significant differences between treatment groups, the experiments were performed as independent triplicates.